Clinical Radiology

Quantitative assessment of myocardial scar heterogeneity using cardiovascular magnetic resonance texture analysis to risk stratify patients post-myocardial infarction

--Manuscript Draft--

Manuscript Number:	CRAD-D-17-00451R2
Full Title:	Quantitative assessment of myocardial scar heterogeneity using cardiovascular magnetic resonance texture analysis to risk stratify patients post-myocardial infarction
Article Type:	Original Paper
Corresponding Author:	Amedeo Chiribiri Kings College London London, UNITED KINGDOM
Corresponding Author Secondary Information:	
Corresponding Author's Institution:	Kings College London
Corresponding Author's Secondary Institution:	
First Author:	Thomas G.J. Gibbs, MBBS, BSc
First Author Secondary Information:	
Order of Authors:	Thomas G.J. Gibbs, MBBS, BSc
	Adriana D.M. Villa, MBBS, MRes
	Eva C. Sammut, MBBS
	Swarna Jeyabraba, MBBS, BSc
	Gerald Carr-White, MBBS, BSc, FRCP, PhD
	Tevfik Ismail, MBBS, PhD
	Gregory Mullen, BSc, PhD
	Balaji Ganeshan, BSc, PhD
	Amedeo Chiribiri
Order of Authors Secondary Information:	

Abstract:	Aim. To determine whether heterogeneity of cardiac scar, as assessed by cardiovascular magnetic resonance texture analysis (CMR-TA), may provide insight into better risk stratification for patients with previous myocardial infarction (MI). Materials and Methods. Patients with previous MI (n=76) were followed for a median of 371.5 days after late gadolinium enhancement (LGE) CMR. The primary endpoint was a composite of ventricular tachycardia, ventricular fibrillation or unexplained syncope. Areas of LGE were identified and manually segmented on a short-axis projection. The characteristics of the scar heterogeneity were evaluated via CMR-TA. This is a filtration-histogram technique, where images are filtered using the Laplacian of a Gaussian filter to extract features different sizes (2-6mm in radius) corresponding to fine, medium and coarse texture scales followed by a quantification step using histogram analysis (skewness and kurtosis). Results. Patients suffering arrhythmic events during the follow-up period demonstrated significantly higher kurtosis (coarse-scale, p=0.005) and lower skewness (fine-scale, p=0.046) compared to those suffering no arrhythmic events. Furthermore, Kaplan Meier analysis showed significantly higher coarse kurtosis (p=0.004), and lower fine skewness (p=0.035) were able to predict increased incidence of ventricular arrhythmic

events.

Conclusions.
In this pilot study, indices of texture analysis reflecting textural heterogeneity were significantly associated with a greater incidence of arrhythmic events. Further work is required to delineate the role of texture analysis techniques in risk stratification post-MI.

1 # Quantitative assessment of myocardial scar heterogeneity

2 # using cardiovascular magnetic resonance texture analysis to

3 # risk stratify patients post-myocardial infarction

4

5 **Thomas Gibbs[1], Adriana D.M Villa[1], Eva Sammut[1], Swarna Jeyabraba[1], Gerald Carr-White[2],**

6 **Tevfik F Ismail[1], Gregory Mullen[1], Balaji Ganeshan[3], Amedeo Chiribiri[1]**

7 **1. School of Biomedical Engineering and Imaging Sciences, King's College London, United Kingdom; 2. Department**
8 **of Cardiology, Guy's and St. Thomas' NHS Foundation Trust, London, United Kingdom; 3. Institute of Nuclear**
9 **Medicine, University College London, United Kingdom**

10

11 **Corresponding author**

12 **Dr Amedeo Chiribiri** MD PhD FHEA

13 Department of Cardiovascular Imaging

14 **King's College London**

15 **School of Biomedical Engineering and Imaging**
16 **Sciences**

17 **4th Floor Lambeth Wing**

18 **St. Thomas' Hospital | London SE1 7EH**

19 Phone: +44(0)20-718-87242

20 Fax: +44(0)20-718-85442

21 Email: amedeo.chiribiri@kcl.ac.uk

22 **Word count: 5,296 (including abstract)**

23

Contributing Author Information

Thomas G. J. Gibbs, Email: thomas.gibbs@kcl.ac.uk

Adriana D. M. Villa, Email: adriana.villa@kcl.ac.uk

Eva C. Sammut, Email: eva.sammut@kcl.ac.uk

Swarna Jeyabraba, Email: swarna.jeyabraba@kcl.ac.uk

Gerald Carr-White, Email: gerry.carr-white@gstt.nhs.uk

Tevfik F Ismail, Email: tevfik.ismail@kcl.ac.uk

Gregory Mullen, Email: greg.mullen@kcl.ac.uk

Balaji Ganeshan, Email: b.ganeshan@ucl.ac.uk

Amedeo Chiribiri, Email: amedeo.chiribiri@kcl.ac.uk

24   *Competing interests*

25   Data analysis and interpretation, and final manuscript preparation were undertaken by the

26   first and last authors, which also act as guarantors for the study. Dr B. Ganeshan is a

27   director, part-time employee and shareholder of Feedback Plc (Cambridge, UK), a company

28   that develops and commercialises the TexRAD texture analysis research software analysis

29   described in this manuscript. None of the other authors report any relevant conflicts of

30   interest.

31

1   **Author Contributions**

2   1.   Guarantor of integrity of the entire study – TG, AC

3   2.   Study concepts and design – TG, AC

4   3.   Literature research - TG

5   4.   Clinical studies – AV, AC, ES

6   5.   Experimental studies / data analysis – TG, AC, TI, BG, SJ

7   6.   Statistical analysis – TG, TI, AC

8   7.   Manuscript preparation – TG, AC

9   8.   Manuscript editing – AV, ES, TI, GCW, GM, SJ

10

EDITOR COMMENTS
Thank you for sending this interesting paper to Clinical Radiology. I am pleased to tell you that it has been recommended for publication providing you respond satisfactorily within three months to the comments at the end of this email.

We are grateful for these comments and we appreciate the opportunity to address the final issues raised by the Reviewer on the manuscript.

REVIEWERS' COMMENTS:

Reviewer #1:

Major Point

1. It is good to see that a multivariable analysis has now been included in the paper to consider the variables in combination. Whilst a brief summary of the results of such analyses have been provided, it would be useful to see further details of the analysis. For example, the hazard ratios and their confidence intervals for the final model used.

Minor Points

None

We agree with the reviewer on the usefulness to report more detailed results for the final model used, and in particular hazard ratios and confidence intervals. These have been added to the Results section of the manuscript (page 9, rows 173-175), as follows (changes are highlighted in red):

Predictors of survival
The Cox model was used to identify factors involved in prediction of survival. When the Cox model including TA parameters significant on univariate analysis were tested and corrected for confounders such as age and LVEF, $kurtosis_{avg}$ at SSF=5 TA and LVEF retained significant independent association with events (p=0.013 and p=0.006, respectively), with hazard ratio of 9.8 (95% confidence interval 1.6-61) for $kurtosis_{avg}$ at SSF=5 TA and 0.95 for LVEF (95% confidence interval 0.92-0.98), respectively. Age and other TA parameters were no longer significant.

Quantitative assessment of myocardial scar heterogeneity using cardiovascular magnetic resonance texture analysis to risk stratify patients post-myocardial infarction

T. Gibbs[1], A. D. M Villa[1], E. Sammut[1], S. Jeyabraba[1], G. Carr-White[2], T. F. Ismail[1], G. Mullen[1], B. Ganeshan[3], A. Chiribiri[1,*]

1. School of Biomedical Engineering and Imaging Sciences, King's College London, UK

2. Department of Cardiology, Guy's and St Thomas' NHS Foundation Trust, London, UK

3. Institute of Nuclear Medicine, University College London, UK

*Guarantor and correspondent: A. Chiribiri, Department of Cardiovascular Imaging, King's College London, School of Biomedical Engineering and Imaging Sciences, 4th Floor Lambeth Wing, St. Thomas' Hospital, London SE1 7EH, UK. Tel.: +44(0)20-718-87242; fax: +44(0)20-718-85442

E-mail address: amedeo.chiribiri@kcl.ac.uk

ABSTRACT

AIM: To determine whether heterogeneity of cardiac scar, as assessed by cardiovascular magnetic resonance (CMR) texture analysis, may provide insight into better risk stratification for patients with previous myocardial infarction (MI).

MATERIALS AND METHODS: Patients with previous MI (*n*=76) were followed for a median of 371.5 days after late gadolinium enhancement (LGE) CMR. The primary endpoint was a composite of ventricular tachycardia, ventricular fibrillation, or unexplained syncope. Areas of LGE were identified and manually segmented on a short-axis projection. The characteristics of the scar heterogeneity were evaluated via CMR texture analysis. This is a filtration-histogram technique, where images are filtered using the Laplacian of a Gaussian filter to extract features different sizes (2–6 mm in radius) corresponding to fine, medium, and coarse texture scales followed by a quantification step using histogram analysis (skewness and kurtosis).

RESULTS: Patients suffering arrhythmic events during the follow-up period demonstrated significantly higher kurtosis (coarse-scale, *p*=0.005) and lower skewness (fine-scale, *p*=0.046) compared to those suffering no arrhythmic events. Furthermore, Kaplan–Meier analysis showed significantly higher coarse kurtosis (*p*=0.004), and lower fine skewness (*p*=0.035) were able to predict increased incidence of ventricular arrhythmic events.

CONCLUSIONS: In this pilot study, indices of texture analysis reflecting textural heterogeneity were significantly associated with a greater incidence of arrhythmic events. Further work is required to delineate the role of texture analysis techniques in risk stratification post-MI.

INTRODUCTION

In recent years, advances in the management of myocardial infarction (MI) have led to significant improvements in patient survival; however, although patients overcome

the index event, many are left with impaired left ventricle (LV) function and carry a risk of life-threatening arrhythmia secondary to impaired LV function and the presence of a myocardial scar. The occurrence of ventricular arrhythmia can result in cardiac arrest and sudden cardiac death (SCD)[1]. Recent guidance recommends implantable cardioverter defibrillator (ICD) implantation for patients deemed at high risk for such events. Currently, ICD is recommended for patients after MI in the presence of significant LV dysfunction;[1,2] however, arrhythmias and SCD are also seen in patients with preserved LV ejection fraction (EF) and the incidence of appropriate shocks in patients receiving an ICD on the basis of current guidelines is low [3]. Therefore, there remains significant debate about how to best identify high-risk patients and avoid the implantation of unnecessary devices. Many patients now routinely undergo cardiac magnetic resonance (CMR) with late gadolinium enhancement (LGE) as part of their evaluation. This test is considered the reference standard for the identification of myocardial scar and fibrosis, and for the quantification of LVEF. Previous data demonstrate that even small areas of scar tissue, which do not impact on LVEF, can result in arrhythmic events, and it has previously been suggested that scar tissue could be a sensitive marker of increased arrhythmic risk [4–6]. On a histopathological level, scar tissue is complex and previous studies using contrast-enhanced CMR delineated two distinct patterns: (1) the scar core, made up of fibrous tissue, characterised by higher signal intensity on LGE images; and (2) heterogeneous tissue, containing necrotic tissue interspersed with bundles of viable myocytes, associated with lower signal intensity compared with the core of the scar [7]. It has been suggested that slow local conduction through these

heterogeneous regions of scar tissue could be responsible for the development of lethal re-entrant arrhythmias [8,9]. Recent studies performed with the aid of numerical simulations have shown that the spatial heterogeneity of fibrosis correlates directly with the risk of arrhythmia and that this is more pronounced with the increase of both the spatial size and the degree of heterogeneity [10].

Quantitative texture analysis (TA) is a tool previously described for the assessment and stratification of solid tumours [11,12]. To the authors' knowledge, TA has not previously been applied to the analysis of CMR images, if preliminary work carried out by the present authors is excluded[13]. CMR-TA has the potential to be applied to the analysis of LGE images, providing additional information on scar heterogeneity [13]. One such TA technique is the filtration-histogram approach where the filtration step extracts and enhances features or objects of different sizes, allowing quantification using histogram-based statistical parameters, which evaluate the grey-level pixel distribution. This filtration-histogram technique has been shown to describe the different components of macroscopic heterogeneity [11]. This is done in terms of standard descriptors, such as mean, standard deviation (SD), skewness, and kurtosis [12,14]. The aim of this exploratory study was to apply quantitative CMR-TA to the assessment of LGE images in patients with previous MI and to determine whether TA-derived indices may provide insights to facilitate better risk stratification in this cohort.

MATERIALS AND METHODS

Patient population

Patients referred on clinical grounds for CMR assessment of myocardial viability were identified retrospectively using electronic hospital records. The study population consisted of consecutive patients who had undergone CMR, with evidence of sub-endocardial or transmural ischaemic scar tissue on LGE imaging. Patients with suspected infiltrative cardiomyopathy (including cardiac haemochromatosis, amyloidosis, or sarcoidosis), myocarditis, or non-ischaemic cardiomyopathies, such hypertrophic cardiomyopathy or dilated cardiomyopathy, were excluded. In order to exclude histologically evolving scar tissue, patients with a recent (<60 days) history of acute coronary syndrome were also excluded. All patients gave written consent to the CMR scan. Local research ethics committee approval was granted (REC 15/NS/003) for retrospective analysis of the data.

CMR imaging protocol

CMR imaging was performed using standardised acquisition protocols using a 1.5 T CMR system with a 32-channel cardiac phased-array surface coil (Philips Healthcare, Best, The Netherlands) [15]. The standard clinical CMR study consisted of a stack of breath-hold short axis cine steady-state free precession sections covering the LV (section thickness of 8 mm and in-plane spatial resolution of 448×448). These were acquired for quantification of LV volumes, function, and mass according to standardised post-processing methods [16]. An inversion-recovery gradient-echo pulse sequence for LGE assessment was used to acquire a stack of short axis sections 15–20 minutes after contrast medium injection (gadobutrol, Bayer-Schering Pharma, Berlin, Germany, 0.2 mmol/kg body weight). Typical acquisition parameters for LGE

imaging were 3.5 ms repetition time (TR), 2 ms echo time (TE), turbo gradient factor of 25, enabling a temporal resolution of 88 ms.

LGE images were used to identify and measure the extent of ischaemic scar tissue (percentage of total LV mass) and for texture analysis post-processing. For this purpose, a commercially available software package was used (CMR42, v5.6.4, Circle Cardiovascular Imaging, Calgary, Canada).

CMR-TA

CMR-TA was performed on LGE images selected at basal, mid-ventricular, and apical level according to standard anatomical positions [15]. Areas of scar at each level were manually segmented and then analysed using TexRAD research software (TexRAD Ltd, Feedback Plc, Cambridge, UK; www.texrad.com). In brief, a region of interest (ROI) was drawn around areas of enhancement ensuring that the scar border but no surrounding tissue was included. The ROI therefore encompassed the scar core and the heterogeneous region. If there were multiple scars in a short axis section, values were averaged together. Manual segmentation of the scar core and heterogeneous region was performed with the consensus of two expert CMR readers blinded to patient identifiers and clinical data.

Images were then filtered using a Laplacian of Gaussian band-pass (similar to a non-orthogonal wavelet approach) filtration step to extract and enhance features of different sizes based on the spatial scale filter (SSF) values varying from 2–6 mm in radius (where 2 mm corresponds to fine texture features, 3–5 mm corresponds to medium texture features, and 6 mm corresponds to coarse texture features; Fig. 1).

Following image filtration, histogram analysis of pixel intensity was performed to quantify each filtered image texture map in terms of statistical parameters such as mean, standard deviation, entropy, skewness, and kurtosis. With this filtration approach, the Gaussian part of the filter reduces the impact of noise component and the Laplacian part enhances subtle features (biologically relevant "heterogeneity") quantifiable by the histogram analysis. These features are potentially relevant for disease diagnosis and prognostic assessment and are not visible to the naked eye on conventional (unfiltered) images. A detailed description of the filtration-histogram technique can be found in the literature [12]. Skewness is a statistical term that describes the asymmetry of a data set from the normal distribution. A negative skewness is where the data points are skewed to the right of a normal bell-shaped curve, whereas a positive skewness involves a leftward skew of the data points. Meanwhile kurtosis quantifies the sharpness of the peak of a frequency–distribution curve. A positive kurtosis indicates a more peaked histogram than a normal distribution, whilst a data-set that is flatter than a normal distribution correlates with a negative kurtosis (Fig. 2). In this study, average, maximum and minimum skewness, and kurtosis were measured in each patient.

Outcome measures and follow-up

Patients were followed up from the point of their initial CMR examination. The primary end-point was a composite of ventricular fibrillation (VF), sustained ventricular tachycardia (VT; defined as VT with a rate >120 beats/min lasting longer

than 30 seconds) with haemodynamic compromise and/or requiring cardioversion, appropriate ICD discharge or unexplained syncope.

Statistical analysis

Continuous variables are expressed as mean±standard deviation (SD), or as median and interquartile range (IQR) in cases where the data were not normally distributed. Categorical data are summarised as frequencies and percentages. The Student's *t*-test was used to compare mean values of continuous data between the group of patients who suffered events and those who did not. Where the data was non-normally distributed, the Mann–Whitney *U*-test was used for group-wise comparison. The relationship of the various imaging and clinical markers with patient survival were assessed using Kaplan–Meier (KM) survival analysis. Only characteristics significantly different between the two groups at the Student's *t*-test or Mann–Whitney test were included in the univariable analysis. This was undertaken to minimise the issue of multiple statistical testing and reduce the false-discovery rates resulting from multiple testing. Optimal thresholds for the above identified texture parameters were determined using receiver operating characteristic (ROC) curve analysis and employed for KM analysis. The log-rank test was employed to assess the difference between the survival distributions. In case of the other clinical and imaging parameters, previously validated thresholds were employed for the KM analysis. KM curves for patients above and below each threshold were constructed to display the proportion of patients surviving at a given time. The survival probability was evaluated according to the factors significant on univariable analysis using the

Cox proportional hazards model. Multivariable analysis was used to adjust for potential confounding. The intra- and interobserver reproducibility of TA was quantified using the intracluster coefficient of correlation.

All data were analysed using Microsoft Excel and IBM SPSS Statistics version 22 for Macintosh, with two-tailed values of $p<0.05$ considered significant.

RESULTS

The study cohort consisted of 76 patients with a median period of follow-up of 371.5 days (IQR 135–645 days). During follow-up, eight patients (10.5%) developed VT, two patients (2.6%) suffered at least one episode of VF, and five patients (6.6%) experienced syncopal events suspected to relate to ventricular arrhythmias, leading to ICD implantation. This comprised a total of 14 patients (18%) with events at follow-up. Baseline characteristics of patients are summarised in Table 1. The mean age of patients was 61.5±11.4 years, 80% were male, 60% had undergone prior revascularisation, and the mean LVEF was 50% (±10%). Five patients had ICD implantation during follow-up and all of these patients were within the events group.

Predictors of adverse events

Baseline characteristics

Patient characteristics related to the primary endpoint are listed in Table 1. There was no significant difference in gender or clinical variables between those who suffered events compared to those who did not, although patients in the event group were significantly older. Furthermore, patients who suffered ventricular arrhythmic

events or unexplained syncope following MI had an on average higher LV end-diastolic volume (EDV), higher end-systolic volume (ESV), larger left atrium (LA), and lower LVEF. Notably, there was no relationship between the total scar burden and occurrence of events.

CMR-TA to assess scar heterogeneity

The median amount of tissue analysed was 2.9 g (IQR, 2–4.3 g) in the events group and 2.7 g (IQR, 1.9–4.5 g) in the group that did not suffer events (p=0.61). Table 2 represents the means ± SD for all the texture parameters employed in the study and their relationship to events on univariable analysis. Patients who had an event had a higher average and maximum kurtosis (kurtosis$_{avg}$ and kurtosis$_{max}$), a trend seen across all filter levels, but only statistically significant in the coarser filter scales, SSF=5 (p=0.007 and 0.005, respectively) and SSF=6 (p=0.015 and 0.025, respectively). Minimum skewness (skewness$_{min}$) at fine filter scale (SSF=2) was found to be significantly lower in the events group (p=0.046).

Survival analysis

Fig. 3 shows KM survival plots based on previously validated thresholds and testing the association between clinical factors and prognosis [17]. Age (>65 years, p=0.03), LVEF (<35%, p=0.048), and indexed LVEDV (>86 ml/m^2, p=0.006) stratified patients for events. LA area (>24 cm^2) was the only factor, amongst those tested, not statistically associated with a higher event rate (p=0.27).

Table 3 and Fig. 4 demonstrate the results from KM analysis only using the texture parameters highlighted above, which significantly differentiated between patients' groups. Specifically, a higher $kurtosis_{max}$ and $kurtosis_{avg}$ value at coarse texture scale (SSF=5 and SSF=6) and lower $skewness_{min}$ value at fine texture scale (SSF=2) predicted poor survival (Table 3).

Interestingly, none of the patients reclassified by TA as low risk had any events, with the exception of one patient in the analysis by $kurtosis_{avg}$ at SSF=5. This was not the case for other significant imaging and clinical markers of survival (e.g., age, LVEF, LA area and LVEDV), where several events occurred in both groups.

Predictors of survival

The Cox model was used to identify factors involved in prediction of survival. When the Cox model including TA parameters significant on univariate analysis were tested and corrected for confounders such as age and LVEF, $kurtosis_{avg}$ at SSF=5 TA and LVEF retained significant independent association with events (p=0.013 and p=0.006, respectively), with hazard ratio of 9.8 (95% confidence interval 1.6–61) for $kurtosis_{avg}$ at SSF=5 TA and 0.95 for LVEF (95% confidence interval 0.92–0.98), respectively. Age and other TA parameters were no longer significant.

Reproducibility analysis

Reproducibly analysis was performed on TA parameters that were associated with events at univariate analysis. Intra-observer reproducibility was excellent for skewness SSF=2 (r=0.96), kurtosis SSF=5 (r=0.99), and kurtosis SSF=6 (r=0.99).

Interobserver reproducibility was good for skewness SSF=2 (r=0.98). Good interobserver reproducibility was measured for kurtosis SSF=5 (r=0.84) and kurtosis SSF=6 (r=0.89).

ROC analysis

ROC curves for TA and standard parameters to the paper are summarised in Table 4. ROC curves for kurtosis$_{avg}$ SSF=5 and LVEF are demonstrated in Fig. 5.

DISCUSSION

Myocardial scar heterogeneity as assessed by CMR-TA is associated with arrhythmic events in patients with previous MI. In particular, a higher kurtosis value at coarse texture scale and lower skewness value at fine texture scale were associated with an adverse outcome. These findings echo the results of previous preliminary work using TA by the present authors' on patients with existing ICDs, which also demonstrated in a different and smaller group of patients that higher kurtosis with application of a coarse filter and lower skewness with application of a fine filter was able to predict post-MI VT or VF [13]. Interestingly, the present data did not show any significant difference in overall scar burden between the event and non-event groups. This possibly suggests that scar heterogeneity assessed by TA could provide independent and complementary information to scar burden, although this hypothesis will have to be tested in future prospective outcome studies. Moreover, the present data confirmed the association between increased age, reduced LVEF, and increased indexed LV EDV with the development of post-MI arrhythmias.

Substantial advances in acute management of myocardial infarction have led to significant improvements in patient survival. Large numbers of these patients are, however, left with impairment of LV function due to myocardial scarring and an increased risk of life-threatening ventricular arrhythmias. Current guidelines focus on LVEF as the key determinant of the need for ICD therapy; however, only the minority of patients who undergo implantation on this basis receive appropriate ICD therapies and, on the other hand, some patients with normal LV function present with arrhythmias or SCD [3]. This has led to significant efforts to refine biomarkers to guide appropriate risk stratification and ICD implantation.

Myocardial scarring in patients with previous MI is accepted as a source of ventricular arrhythmias [9,18]. Previous data demonstrated that even small areas of scar, which do not impact on LVEF, can result in arrhythmic events [4,5]. Bello *et al* [19] was the first to directly analyse the relationship between some morphological features of myocardial scar and the induction of ventricular arrhythmia. Scar surface and mass, as characterised by CMR, were shown to be better predictors of inducible monomorphic VT than LVEF [19]. This study, however, did not provide any insight into the role of scar heterogeneity.

Electrical mapping studies have shown that the border areas of infarcted myocardial tissue, found adjacent to dense scars, are responsible for this arrhythmogenicity [7,9,20]. This area, also known as grey zone, is a heterogeneous region composed of isolated bundles of viable myocytes interwoven with fibrous tissue [21]. Grey zone regions conduct electrical activity more slowly than the surrounding myocardium, leading to the development of re-entrant VT [9,22,23].

Subsequent studies have shown that more extensive grey zone at the periphery of a scar strongly correlates with greater VT inducibility, and that the extent of grey zone provides incremental prognostic value beyond LVEF [24]. More recently the same findings have been made in spontaneous VT following myocardial infarction [25]. These studies provide powerful evidence that factors, other than the presence and extent of scarring, play a pivotal role in the pathogenesis of ventricular arrhythmias.

The current study is the first to go beyond the assessment of the extent of the grey zone and to consider the make-up of the heterogeneous infarct area itself, testing the hypothesis that scar complexity is linked to the development of arrhythmias. TA was initially developed in the field of oncology, where the complexity of solid tumour tissue has been shown to predict prognosis, assess disease severity, and treatment response evaluation [11]. The present study demonstrates for the first time *in vivo* that specific features of the texture of the scar are linked to arrhythmogenicity. The same features have been previously associated with increased risk of arrhythmic events in pathological and computational modelling studies [10]. The present findings are in keeping with current understanding of the pathophysiological mechanisms linking the presence of scarring to the onset of re-entrant arrhythmias.

The interpretation of the biological meaning of the observed values of skewness and kurtosis has been previously published in the literature [12]. Higher kurtosis values indicate increased visual contrast (intensity variation) in the objects highlighted by filtration in relation to the background tissue. A lower skewness value indicates the presence of darker areas. In combination, these features suggest a more heterogeneous scar, comprising areas of grey zone interspersed with areas of

denser scar. Interestingly, there was no significant difference between the two groups in terms of scar burden, probably indicating that these texture features of scar heterogeneity could provide independent information from the presence or absence and the burden of scar.

The present findings are in keeping with recent data investigating the role of scar heterogeneity in the genesis of arrhythmia by means of mathematical models. This study assessed the role of mean fibrosis level and of the extent and spatial size of the heterogeneity and demonstrated that a more heterogeneous distribution of fibrosis was associated with an increased likelihood of arrhythmias and that the main mechanism of this dependency was the presence of localised tissue patches with more severe degrees of fibrosis [10].

LGE images were acquired in this study according to standard clinical practice and SCMR guidelines, with a relatively short acquisition time in order to limit the amount of motion [15]. This is a particularly important aspect as motion could potentially result in the inclusion of blood-pool in the ROI, particularly when small subendocardial scars are analysed, or might contribute to a loss of information when finer texture is analysed. A significant improvement on this side will be allowed by the advent of a new generation of sequences for "dark-blood" LGE, which may further improve scar conspicuity [26,27].

This is a pilot study to assess the potential for TA to be used as an added marker of risk and estimate the effect size in view of future adequately powered studies to test an independent association between scar texture features and events. The present results suggest excellent predictive abilities for events using TA parameters;

however, optimised cut-off values were used based on ROC analysis as this was a pilot exploratory study, whereas cut-off values from the literature were used for the evaluation of standard markers of risk, likely resulting in a relative underestimation of the predictive ability of the latter. Multivariable Cox regression analysis was included in the present and demonstrated the presence of an independent association between TA (kurtosis SSF=5 average) and events. Given the pilot nature of this study and the relatively limited sample size, these findings will need to be confirmed by a future prospective study on a larger population of patients.

The use of texture analysis in addition to standard clinical and functional data derived from CMR such as the presence of scar and LVEF (e.g., a multi-parametric approach) may provide additional information to guide risk stratification of patients post-myocardial infarction.

ACKNOWLEDGEMENTS

REFERENCES

1 Moss AJ, Zareba W, Hall WJ, *et al.* Prophylactic implantation of a defibrillator in patients with myocardial infarction and reduced ejection fraction. *N Engl J Med* 2002; 346: 877–83.

2 Bardy GH, Lee KL, Mark DB, *et al.* Amiodarone or an implantable cardioverter-defibrillator for congestive heart failure. *N Engl J Med* 2005; 352: 225–37.

3 Buxton AE. Identifying the high risk patient with coronary artery disease--is ejection fraction all you need? *J Cardiovasc Electrophysiol* 2005; 16(Suppl. 1): S25-27.

4 Kwong RY, Chan AK, Brown KA, *et al.* Impact of unrecognized myocardial scar detected by cardiac magnetic resonance imaging on event-free survival in patients presenting with signs or symptoms of coronary artery disease. *Circulation* 2006; 113: 2733–43.

5 Kwong RY, Sattar H, Wu H, *et al.* Incidence and prognostic implication of unrecognized myocardial scar characterized by cardiac magnetic resonance in diabetic patients without clinical evidence of myocardial infarction. *Circulation* 2008; 118: 1011–20.

6 Chen Z, Sohal M, Voigt T, *et al.* Myocardial tissue characterization by cardiac magnetic resonance imaging using T1 mapping predicts ventricular arrhythmia in ischemic and non–ischemic cardiomyopathy patients with implantable cardioverter–defibrillators. *Heart Rhythm* 2015; 12: 792–801.

7 Schmidt A, Azevedo CF, Cheng A, *et al.* Infarct tissue heterogeneity by magnetic resonance imaging identifies enhanced cardiac arrhythmia susceptibility in patients with left ventricular dysfunction. *Circulation* 2007; 115: 2006–14.

8 Verma A, Marrouche NF, Schweikert RA, *et al.* Relationship between successful ablation sites and the scar border zone defined by substrate mapping for ventricular tachycardia post-myocardial infarction. *J Cardiovasc Electrophysiol* 2005; 16: 465–71.

9 de Bakker JM, van Capelle FJ, Janse MJ, *et al.* Reentry as a cause of ventricular tachycardia in patients with chronic ischemic heart disease: electrophysiologic and anatomic correlation. *Circulation* 1988; 77: 589–606.

10 Kazbanov IV, ten Tusscher KHWJ, Panfilov AV. Effects of heterogeneous diffuse fibrosis on arrhythmia dynamics and mechanism. *Sci Rep* 2016; Feb 10;6:20835. doi: 10.1038/srep20835.

11 Davnall F, Yip CSP, Ljungqvist G, *et al.* Assessment of tumor heterogeneity: an emerging imaging tool for clinical practice? *Insights Imaging* 2012; 3: 573–89.

12 Miles KA, Ganeshan B, Hayball MP. CT texture analysis using the filtration-histogram method: what do the measurements mean? *Cancer Imaging Off Publ Int Cancer Imaging Soc* 2013; 13: 400–6.

13 Ali N, Mullen G, Chiribiri A. Risk stratification of post-MI patients for ICD implantation using texture analysis to quantify heterogeneity of scar. *J Cardiovasc Magn Reson* 2015; 17: Q14.

14 Ganeshan B, Miles KA. Quantifying tumour heterogeneity with CT. *Cancer Imaging Off Publ Int Cancer Imaging Soc* 2013; 13: 140–9.

15 Kramer CM, Barkhausen J, Flamm SD, Kim RJ, Nagel E, Society for Cardiovascular Magnetic Resonance Board of Trustees Task Force on Standardized

Protocols. Standardized cardiovascular magnetic resonance (CMR) protocols 2013 update. *J Cardiovasc Magn Reson Off J Soc Cardiovasc Magn Reson* 2013; 15: 91.

16   Schulz-Menger J, Bluemke DA, Bremerich J, *et al.* Standardized image interpretation and post processing in cardiovascular magnetic resonance: Society for Cardiovascular Magnetic Resonance (SCMR) board of trustees task force on standardized post processing. *J Cardiovasc Magn Reson Off J Soc Cardiovasc Magn Reson* 2013; 15: 35.

17   Hudsmith LE, Petersen SE, Francis JM, Robson MD, Neubauer S. Normal human left and right ventricular and left atrial dimensions using steady state free precession magnetic resonance imaging. *J Cardiovasc Magn Reson Off J Soc Cardiovasc Magn Reson* 2005; 7: 775–82.

18   Richards DA, Blake GJ, Spear JF, Moore EN. Electrophysiologic substrate for ventricular tachycardia: correlation of properties *in vivo* and *in vitro*. *Circulation* 1984; 69: 369–81.

19   Bello D, Fieno DS, Kim RJ, *et al.* Infarct morphology identifies patients with substrate for sustained ventricular tachycardia. *J Am Coll Cardiol* 2005; 45: 1104–8.

20   Horowitz LN, Harken AH, Kastor JA, Josephson ME. Ventricular resection guided by epicardial and endocardial mapping for treatment of recurrent ventricular tachycardia. *N Engl J Med* 1980; 302: 589–93.

21   Chen Z, Sohal M, Voigt T, *et al.* Myocardial tissue characterization by cardiac magnetic resonance imaging using T1 mapping predicts ventricular arrhythmia in ischemic and non-ischemic cardiomyopathy patients with implantable cardioverter–defibrillators. *Heart Rhythm Off J Heart Rhythm Soc* 2015; 12: 792–801.

22   Ursell PC, Gardner PI, Albala A, Fenoglio JJ, Wit AL. Structural and electrophysiological changes in the epicardial border zone of canine myocardial infarcts during infarct healing. *Circ Res* 1985; 56: 436–51.

23   Dillon SM, Allessie MA, Ursell PC, Wit AL. Influences of anisotropic tissue structure on reentrant circuits in the epicardial border zone of subacute canine infarcts. *Circ Res* 1988; 63: 182–206.

24   Yan AT, Shayne AJ, Brown KA, *et al.* Characterization of the peri-infarct zone by contrast-enhanced cardiac magnetic resonance imaging is a powerful predictor of post-myocardial infarction mortality. *Circulation* 2006; 114: 32–9.

25   Roes SD, Borleffs CJW, van der Geest RJ, *et al.* Infarct tissue heterogeneity assessed with contrast-enhanced MRI predicts spontaneous ventricular arrhythmia in patients with ischemic cardiomyopathy and implantable cardioverter-defibrillator. *Circ Cardiovasc Imaging* 2009; 2: 183–90.

26   Holtackers RJ, Chiribiri A, Schneider T, Higgins DM, Botnar RM. Dark-blood late gadolinium enhancement without additional magnetization preparation. *J Cardiovasc Magn Reson Off J Soc Cardiovasc Magn Reson* 2017; 19: 64.

27   Peel SA, Morton G, Chiribiri A, Schuster A, Nagel E, Botnar RM. Dual inversion-recovery MR imaging sequence for reduced blood signal on late gadolinium-enhanced images of myocardial scar. *Radiology* 2012; 264: 242–9.

Figure 1: TA filtration technique. LGE-enhanced CMR image with the myocardial scar and corresponding images selectively displaying fine (SSF 2), medium (SS4) and coarse (SSF5) lesion texture, respectively. These varying textures correspond to

myocardial scar features of different sizes and intensity variations extracted by the image filter.

Figure 2: (a) Graphs demonstrating a negative and positive skewed histogram. Skewness is a measure of the asymmetry of a distribution. The skewness value can be positive or negative. Negative skew indicated that the tail on the left side of the histogram is longer or fatter than the right side. Positive skew indicates that the tail is longer or fatter on the right side than the left side. A zero value occurs when the tails either side of the mean balance out, indicating an even distribution. (b) An illustration of positive and negative kurtosis compared to a normal distribution. Kurtosis is a measure of the peakedness of a distribution. The kurtosis value can be positive or negative. In comparison to a normal (Gaussian) distribution, a positive kurtosis indicates a more peaked histogram. A negative kurtosis correlates with a flatter histogram than that of a Gaussian distribution.

Figure 3: KM analysis of standard parameters of arrhythmic risk. The difference in event-free survival when patients are stratified according to previously validated thresholds for age, left atrium size, LVEDV/m^2, and LVEF are demonstrated.

Figure 4: KM survival analysis of texture analysis parameters. KM curves demonstrate the difference in event-free survival when patients are stratified according to average kurtosis when SSF5 (a) and SSF6 (b) filter levels are applied; maximum kurtosis when SSF5 (c) and SSF6 (d) are applied; and minimum skewness when SSF2 (e) is applied. The thresholds used to stratify patients are optimised cut-offs from ROC analysis.

Figure 5: ROC curves for kurtosis SSF5 average and LVEF.

Table 1: Demographics and baseline cardiovascular magnetic resonance characteristics.

Characteristic	All patients (*N*=76)	Ventricular arrhythmia or unexplained syncope (*n*=14)	No ventricular arrhythmia or unexplained syncope (*n*=62)	*p*-Value
Age (years)	61.51±11.4	67.9±10	60.1±12	0.01
Male	66 (80%)	13 (93%)	53 (85%)	0.4
Clinical history				
Diabetes mellitus	21 (28%)	4 (29%)	17 (27%)	0.96
Hypertension	58 (76%)	11 (79%)	47 (76%)	0.78
Cigarette smoker	19 (25%)	3 (21%)	16 (26%)	0.60
Hypercholesterolaemia	47 (62%)	10 (71%)	37 (60%)	0.45
Atrial fibrillation	9 (12%)	1 (7%)	8 (13%)	0.48
Prior revascularisation				
CABG	12 (16%)	3 (21%)	9 (15%)	0.61
PCI	42 (55%)	7 (50%)	35 (56%)	0.59
Cardiac MRI				
Scar burden (% of LV mass)	4.2±2.4	4.9±2.3	4±2.4	0.24
LVEF (%)	51.8 (42.5-61.8)	44.5 (25.7-51.2)	54.6 (44.3-62.1)	0.01
LVEDV (ml)	175.4 (140.3-212)	202.5 (179-261.5)	170 (133.5-207.5)	0.02
LVEDV/m^2	86.5 (76.3-107)	106 (90-125.3)	83 (75.3-100.3)	0.01
LVESV (ml)	82 (56.3-119)	106.5 (82-177.5)	73.5 (51.8-114)	0.01
LVESV/m^2	39.5 (29-58.8)	55.5 (43.1-88)	35.5 (27.8-54.8)	0.01
LV mass (g)	105.7±46.7	112.4±54.2	103.9±45.1	0.59
LV mass/m^2	60.4±16.4	66.9±19.4	58.9±15.5	0.19
RVEF (%)	58.2 (51.5-63)	57.7 (46.6-65.4)	58.5 (51.6-63)	0.74
RVEDV (ml)	148 (121.3-	143.5 (115.5-	150 (121.8-	0.88

	173)	173.8)	173.3)	
RVEDV/m^2	75 (61.3-87)	71 (58-97.8)	76 (62-86.3)	0.96
RVESV (ml)	62 (46.3-81.8)	41 (42.8-89.8)	62 (47.8-79.5)	0.79
RVESV/m^2	31 (22-39.5)	31 (21-43.7)	31 (24-40)	0.81
LA (cm^2)	25.1±5.8	27.6±4.2	24.5±5.9	0.03
RA (cm^2)	27.9±44.8	23.1±5.5	29±49.6	0.36

Values are mean plus or minus standard deviation, median and interquartile range or *n* (%). *p*-Value pertains to the comparison between groups with and without ventricular arrhythmia/unexplained syncope events.

CABG, coronary artery by-pass graft; PCI, percutaneous coronary intervention; MRI, magnetic resonance imaging; LVEF , left ventricular ejection fraction; EDV , end-diastolic volume; ESV, end-systolic volume; RVEF, right ventricular ejection fraction; LA, left atrium; RA, right atrium.

Table 2: Detailed results of cardiovascular magnetic resonance texture analysis (CMR-TA) for SSF of 2 to 6.

Statistical parameters	All patients (*N*=76)	Ventricular arrhythmia or unexplained syncope (*n*=14)	No ventricular arrhythmia or unexplained syncope (*n*=62)	*p*-Value
SSF2				
Mean intensity	247.3±169.4	244.5±222.36	247.9±157.4	0.960
Standard deviation	542.5±280.5	430.9±249.6	567.7±282.8	0.085
Entropy	6±0.6	5.9±0.4	6±0.7	0.400
Mean of positive pixels	550.4±283.7	460±285.7	570.8±281.5	0.204
Skewness$_{max}$	0.3±0.3	0.2±0.3	0.3±0.3	0.274
Skewness$_{avg}$	0.2±0.3	0.1±0.2	0.2±0.3	0.068
Skewness$_{min}$	0.1±0.3	-0.1±0.2	0.1±0.3	0.046
Kurtosis$_{max}$	0.1±0.6	0.2±0.6	0.1±0.7	0.488
Kurtosis$_{avg}$	-0.1±0.5	0±0.3	-0.1±0.5	0.762
Kurtosis$_{min}$	-0.3±0.5	-0.3±0.3	-0.3±0.5	0.962

SSF3				
Mean intensity	304.5±245.8	343.4±301.2	295.7±233.5	0.586
Standard deviation	593.9±314.6	474.3±299.1	621±314	0.116
Entropy	6±0.63	5.9±0.4	6±0.7	0.415
Mean of positive pixels	629.7±336.2	554.2±363.1	646.8±330.5	0.392
$Skewness_{max}$	0.2±0.3	0.2±0.3	0.2±0.3	0.754
$Skewness_{avg}$	0.1±0.3	0±0.3	0.1±0.3	0.537
$Skewness_{min}$	-0.1±0.4	-0.2±0.4	0±0.4	0.350
$Kurtosis_{max}$	0±0.6	0.2±0.7	0±0.6	0.287
$Kurtosis_{avg}$	-0.2±0.5	0±0.6	-0.2±0.4	0248
$Kurtosis_{min}$	-0.3±0.5	-0.2±0.7	-0.4±0.5	0.276
SSF4				
Mean intensity	306.7±312.8	394.2±347.8	287±304	0.301
Standard deviation	606.6±324.1	486.4±314.7	633.8±322.5	0.131
Entropy	6±0.6	5.9±0.4	6±0.7	0.415
Mean of positive pixels	647.5±360.3	601.8±402.8	657.9±352.7	0.636
$Skewness_{max}$	0.1±0.4	0.2±0.4	0.1±0.4	0.398
$Skewness_{avg}$	-0.1±0.3	0±0.3	-0.1±0.3	0.557
$Skewness_{min}$	-0.2±0.4	-0.2±0.4	-0.2±0.3	0.994
$Kurtosis_{max}$	-0.1±0.7	0.2±0.5	-0.1±0.7	0.074
$Kurtosis_{avg}$	-0.3±0.4	-0.1±0.5	-0.4±0.4	0.056
$Kurtosis_{min}$	-0.5±0.4	-0.3±0.6	-0.5±0.4	0.108
SSF5				
Mean intensity	279.2±367.6	408.2±370.3	250±363.7	0.163
Standard deviation	609.7±328.1	483.7±310	638.2±327.7	0.111
Entropy	6±0.6	5.9±0.4	6±0.7	0.444
Mean of positive pixels	646.7±373.6	613.2±416.1	654.2±366.6	0.737
$Skewness_{max}$	0±0.4	0.1±0.4	0±0.4	0.570
$Skewness_{avg}$	-0.1±0.3	-0.1±0.3	-0.1±0.3	0.732
$Skewness_{min}$	-0.3±0.3	-0.3±0.4	-0.3±0.3	0.865
$Kurtosis_{max}$	-0.2±0.5	0±0.3	-0.3±0.5	0.005
$Kurtosis_{avg}$	-0.4±0.4	-0.2±0.3	-0.5±0.4	0.007
$Kurtosis_{min}$	-0.6±0.4	-0.4±0.4	-0.7±0.4	0.052
SSF6				
Mean intensity	239.9±409.4	398±376.4	204.2±410.9	0.102
Standard deviation	605±332.2	476.4±300.4	634.1±334.3	0.097
Entropy	6±0.6	5.9±0.4	6±0.7	0.540
Mean of	631.7±382	607.2±417.9	637.2±376.9	0.808

positive pixels				
Skewness$_{max}$	0±0.4	-0.1±0.4	0±0.4	0.713
Skewness$_{avg}$	-0.1±0.3	-0.2±0.4	-0.2±0.3	0.665
Skewness$_{min}$	-0.3±0.3	-0.4±0.4	-0.3±0.4	0.511
Kurtosis$_{max}$	-0.2±0.5	-0.1±0.4	-0.4±0.5	0.025
Kurtosis$_{avg}$	-0.4±0.4	-0.3±0.3	-0.6±0.3	0.015
Kurtosis$_{min}$	-0.6±0.4	-0.5±0.4	-0.7±0.3	0.075

Values are mean plus or minus standard deviation. *p*-Value pertains to the comparison between groups with and without ventricular arrhythmia/unexplained syncope events.

SSF, spatial scale filter.

Table 3: Log rank results.

	Log rank	*p*-Value	ROC analysis threshold	No. of patients assigned to the low-risk group by CMR-TA	No. of patients assigned to the high-risk group by CMR-TA
SSF2					
Skewness$_{min}$	4.460	0.035	0.120	25	51
SSF5					
Kurtosis$_{max}$	5.319	0.021	-0.445	53	23
Kurtosis$_{avg}$	6.397	0.011	-0.493	45	31
SSF6					
Kurtosis$_{max}$	8.407	0.004	-0.465	47	29
Kurtosis$_{avg}$	6.343	0.012	-0.628	51	25

Log rank, *p*-value, optimised thresholds and number of patients within the low and high risk group are shown, as stratified according to each TA-CMR parameter.

CMR-TA, cardiovascular magnetic resonance texture analysis; SSF, spatial scale filter.

Table 4: ROC analysis for different predictors of outcome.

Test result variables	Area	SE	p-Value	Asymptotic 95% confidence interval	
				Lower bound	Upper bound
Age	0.7	0.075	0.02	0.554	0.847
LVEF	0.715	0.082	0.012	0.554	0.876
Kurtosis$_{avg}$ SSF=5	0.73	0.064	0.008	0.605	0.855
Kurtosis$_{max}$ SSF=5	0.729	0.063	0.008	0.604	0.853
Kurtosis$_{min}$ SSF=5	0.654	0.077	0.073	0.504	0.805
Kurtosis$_{avg}$ SSF=6	0.715	0.066	0.012	0.586	0.845
Kurtosis$_{max}$ SSF=6	0.705	0.063	0.017	0.582	0.828
Kurtosis$_{min}$ SSF=6	0.656	0.079	0.07	0.5	0.811
Skewness$_{avg}$ SSF=2	0.589	0.089	0.299	0.415	0.763
Skewness$_{max}$ SSF=2	0.586	0.087	0.318	0.415	0.757
Skewness$_{min}$ SSF=2	0.594	0.076	0.275	0.445	0.742

Detailed results of received operating characteristics curves for different predictors of outcome identified by univariable analysis.

SE, standard error; SSF, spatial scale filter; LVEF, left ventricular ejection fraction.

Figure 1

Unfiltered image (SSF0)
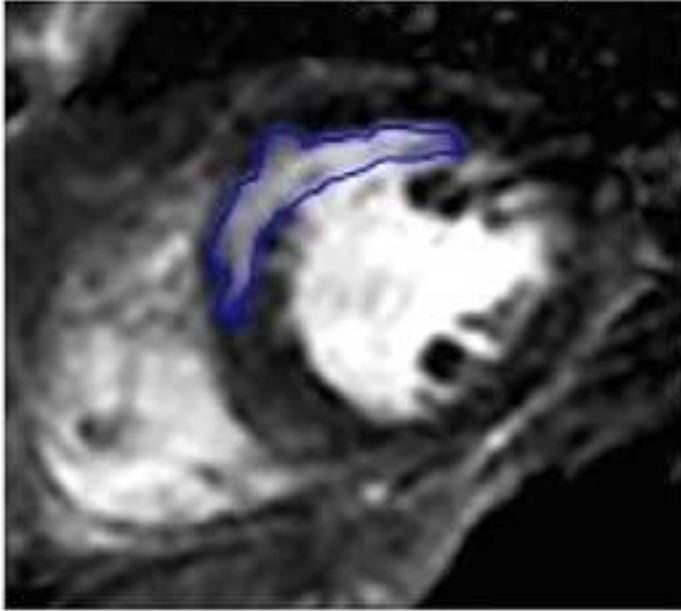
Fine texture (SSF2)
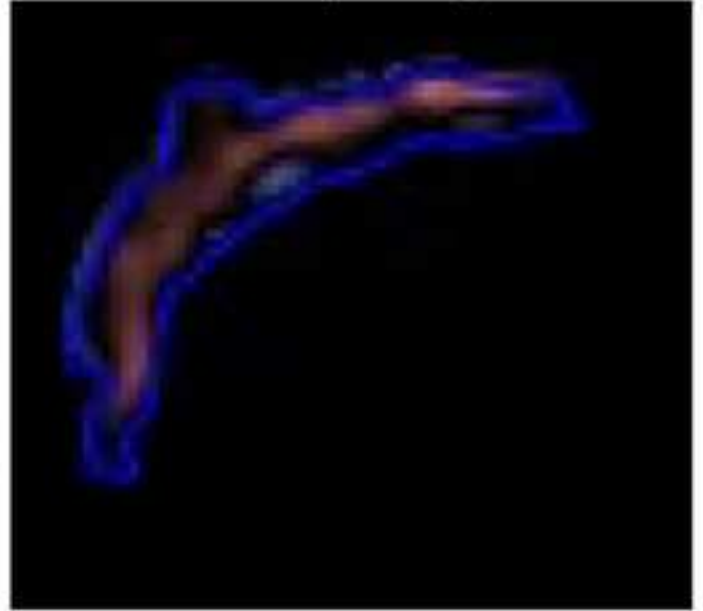
Medium texture (SSF4)

Coarse texture (SSF6)

Figure 2

Figure 3

Figure 4 NEW

Figure 5 NEW
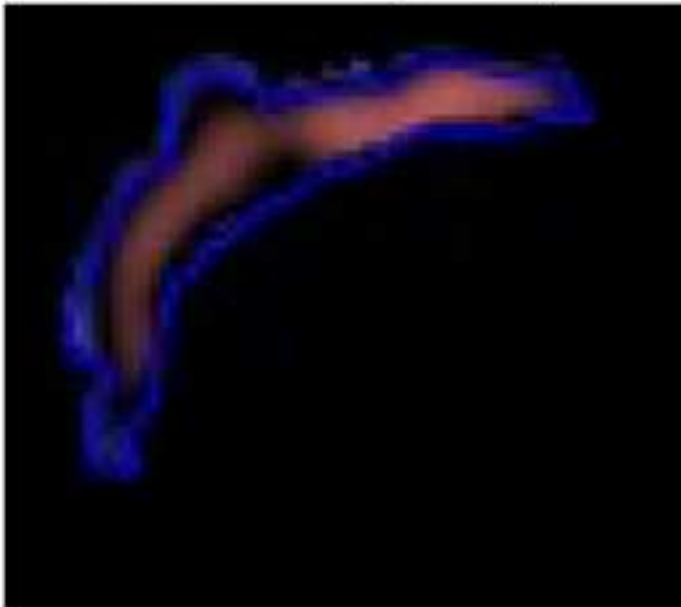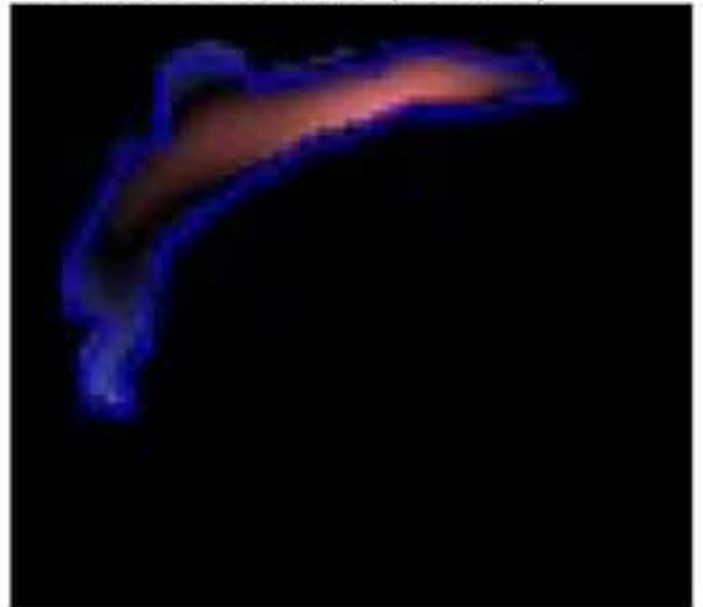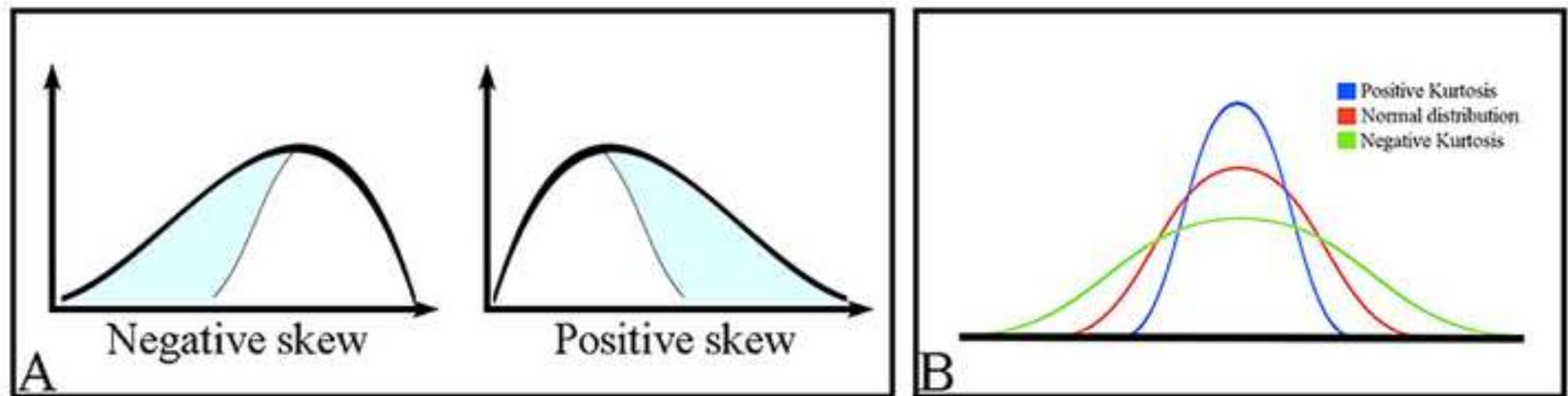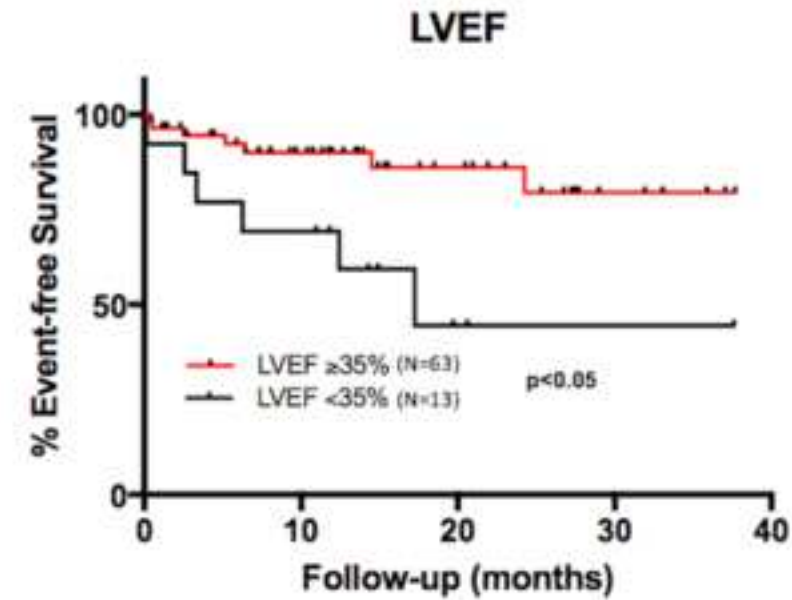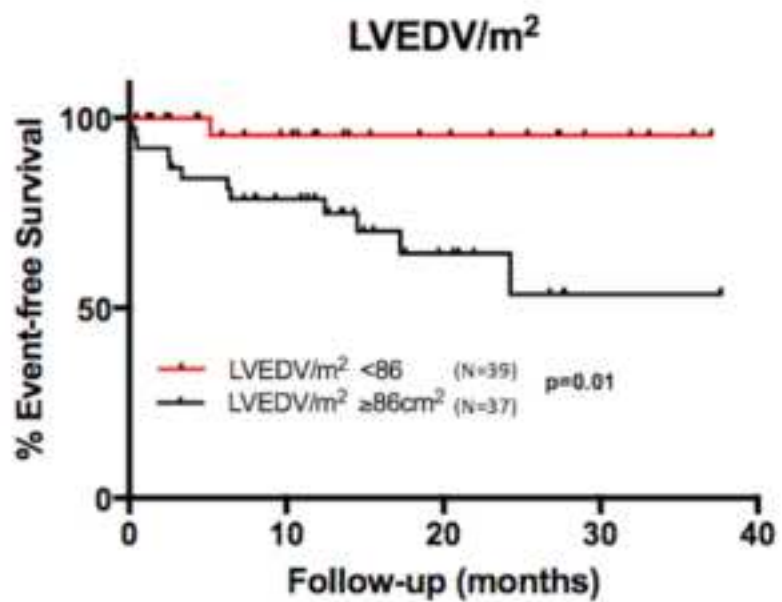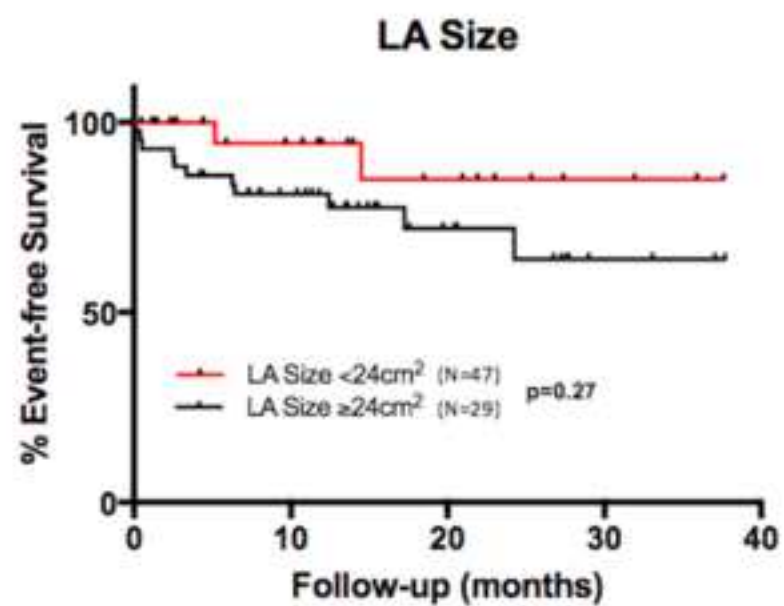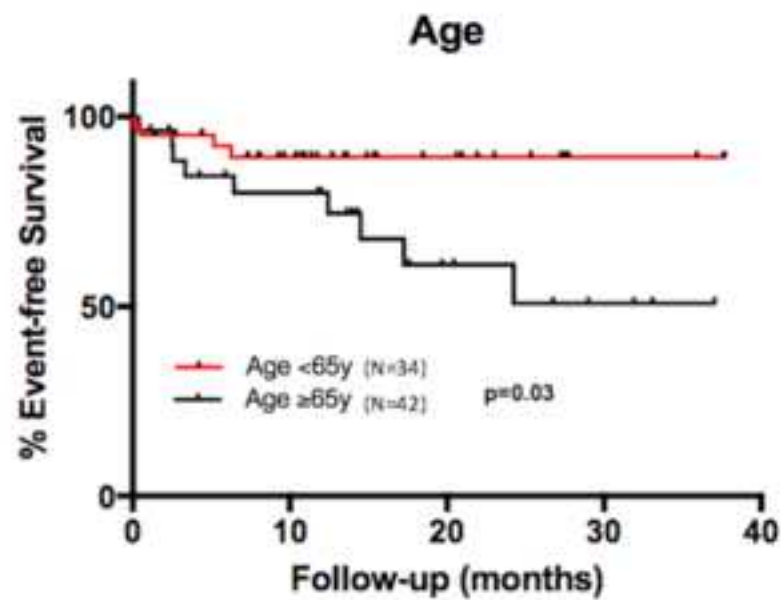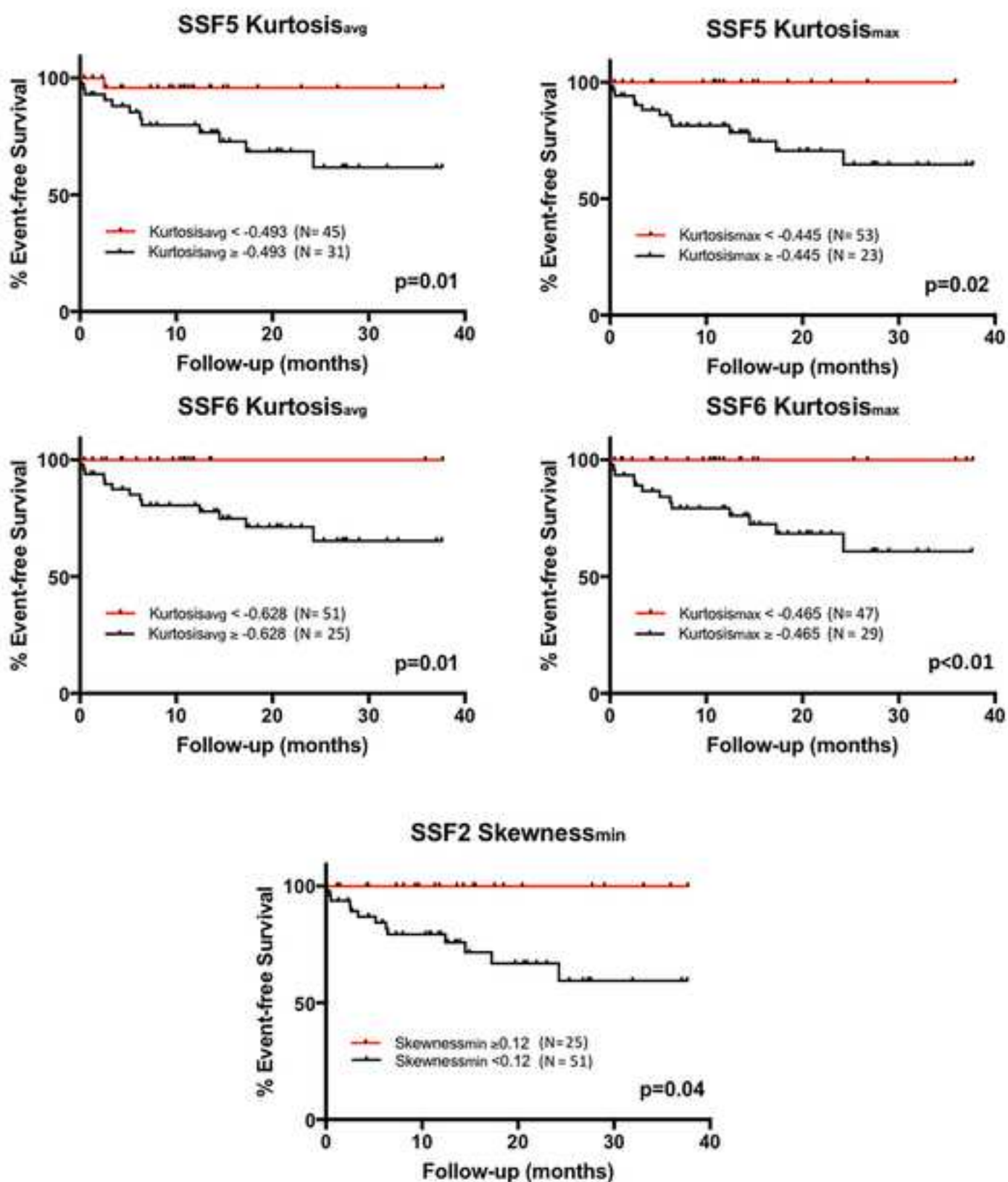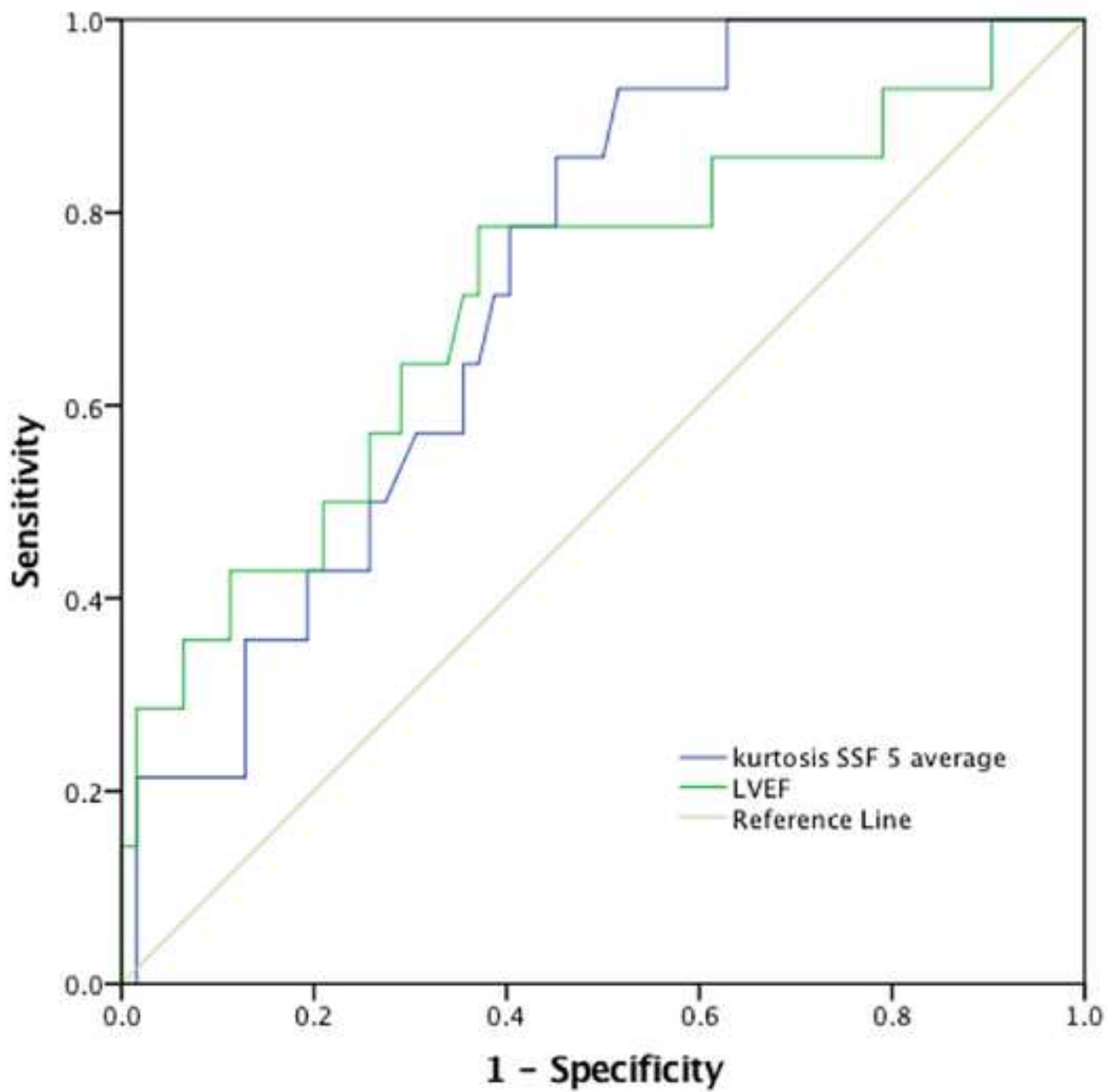
1 **Highlights**

2 • Texture analysis indices are associated with increased incidence of arrhythmias
3 • Predictive texture features correspond biologically to more heterogenous scar
4 • Scar heterogeneity may aid risk-stratification after myocardial infarction